Controlled Evolution of Carbon Nanotubes Coated by Nanodiamond: the Realization of a New Class of Hybrid Nanomaterials

M. L. Terranova,* S. Orlanducci, A. Fiori, E. Tamburri, and V. Sessa

Dipartimento di Scienze e Tecnologie Chimiche and MINASlab, University of Rome Tor Vergata, Via della Ricerca Scientifica, 00133 Roma, Italy

M. Rossi

Dipartimento di Energetica, University of Rome La Sapienza, Via A. Scarpa 14, 00161 Roma, Italy

A. S. Barnard

Center for Nanoscale Materials, Argonne National Laboratory, 9700 South Cass Avenue, Argonne, Illinois, 60439

Received January 28, 2005. Revised Manuscript Received April 1, 2005

We report a new class of nanostructured carbon materials, which couple nanosized diamond with single-walled carbon nanotubes. This exciting material is being produced in our laboratories in a modified CVD reactor by means of reactions between carbon nanopowders and atomic H. Field-emission scanning electron microscopy (FE-SEM), transmission electron microscopy (TEM), Raman spectroscopy, and reflection high-energy electron diffraction (RHEED) have been used to study samples grown for various deposition times. The information achieved by combined use of these characterization techniques has enabled the construction of a time-growth sequence for the two carbon nanophases and has enlightened the peculiar growth of such hybrid carbon systems. The tubular inner structures are found to be bundles of single-walled carbon nanotubes (SWNT) up to 15 μm long, and the outer deposits consist of well-shaped diamond crystallites with diameters in the 20−100 nm range. The one-step synthesis approach described here provides an experimental route to the production of ordered arrays of rigid nanotubes coated by diamond nanocrystallites.

Introduction

The increasing scale of device integration in solid-state technology coinciding with decreasing structure dimensions requires the use of nanomaterials that can be fabricated into net shapes. Moreover, to realize the full potential of the new technologies, the material itself must survive under significantly severe environmental conditions. In this context the family of carbon nanostructures, with outstanding mechanical, chemical, and thermal properties, is ideally suited to a wide range of innovative applications. This family includes nonplanar nanographites, such as nanotubes, but also diamond particles with dimension less than a few hundreds of nanometers.[1]

On the other hand, the challenge to take meaningful advantage of the extreme properties of nanocrystalline diamond and the tendency toward fabrication of one- or quasi-one-dimensional nanostructures have stimulated recent investigations on the properties foreseen for diamond in the form of tubular nanosystems, such as nanowires or nanorods.

Using ab initio techniques[2−4] the structural and energetic stability of diamond nanowires has been studied as a function of the surface morphology and crystallographic direction of the principal axis.

Another study based on ab initio data compared the mechanical properties of carbon nanotubes with those predicted for an equivalent diamond nanorod.[5] Interestingly, the theoretical and computational results suggested that a diamond nanorod might exhibit mechanical performances superior to those of carbon nanotubes at certain sizes.

Furthermore, a thermodynamic model predicts an energetic stability for diamond nanowires that may be equivalent to that of carbon nanotubes in certain size regimes;[6] and an alternative thermodynamic approach performed in ref 7 indicated that nucleation of diamond would be preferable inside a carbon nanotube compared with a flat substrate. On

* To whom correspondence should be addressed. E-mail: terranova@roma2.infn.it.

(1) Shenderova, O. A.; Zhirnov, V. V.; Brenner, D. W. *Crit. Rev. Solid State Mater. Sci.* **2002**, *27*, 227.
(2) Barnard, A. S.; Russo, S. P.; Snook, I. K. *Nano Lett.* **2003**, *10*, 1323.
(3) Barnard, A. S.; Russo, S. P.; Snook, I. K. *Philos. Mag.* **2004**, *84*, 899.
(4) Barnard, A. S.; Russo, S. P.; Snook, I. K. *Nanosci. Nanotechnol.* **2004**, *4*, 151.
(5) Shenderova, O.; Brenner D.; Ruoff, R. *Nano Lett.* **2003**, *3*, 805.
(6) Barnard, A. S.; Snook, I. K. *J. Chem. Phys.* **2004**, *120*, 3817.
(7) Liu, Q. X.; Wang, C. X.; Li, S. W.; Zhang, J. X.; Wu Yang, G. *Carbon* **2004**, *42*, 629.

10.1021/cm0502018 CCC: $30.25
Published on Web 05/05/2005

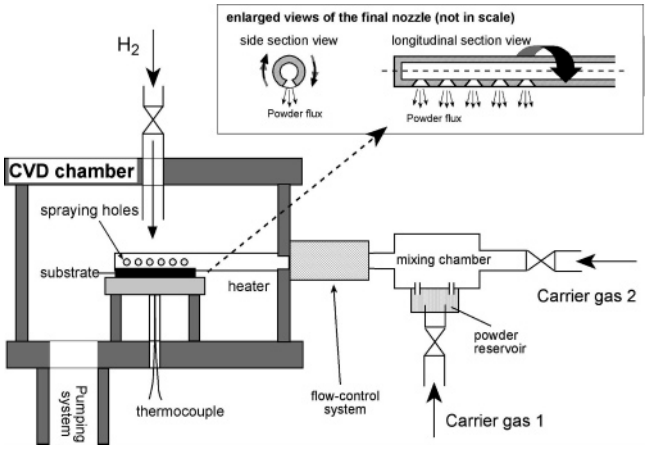

Figure 1. Schematic drawing of the HF−CVD reactor set up. The inset shows an enlarged view of the final nozzle used to spray the nanocarbon particle onto the substrate surface.

this basis the authors predicted that carbon nanotubes would be an effective path to grow diamond nanowires.

Up to now, however, only a few examples of tubular diamond-based nanosystems have been produced. We can cite the nanowhiskers and nanorods obtained by microfabrication methods involving RIE of single crystalline diamond,[8−9] homoepitaxially grown single-crystal diamond nanorods and RIE-generated nanowhiskers,[10] nanocylinders (about 300 nm diameter) produced by CVD using a templating method,[11] and vertically aligned single-crystal nanotubular diamond structures grown using MPECVD.[12] Recent studies[13,14] reported the transformation, induced by H plasma treatments, of multiwalled carbon nanotubes into rows of nanocrystalline diamond and suggested a new route to the production of cylindrically shaped distributions of diamond nanocrystallites.

In the course of research dealing with production of carbon nanostructures by CVD techniques we noted that, under well-defined conditions, it was possible to generate during the same run a most exciting combination of carbon nanotubes and nanocrystalline diamond. In this paper we provide evidence of fascinating nucleation and growth features that dictate the building of rigid nanocylindrical structures formed by single-walled carbon nanotubes (SWCNT) completely covered by nanosized diamond.

Experimental Section

The deposition experiments have been carried out in a hot-filament CVD reactor connected to a purpose-designed powder-flowing apparatus, schematically reported in Figure 1. As in our previous experiments devoted to the production of carbon nanotubes,[15] the reactants were carbon nanopowders (mean diameter 40 nm) produced by cw-laser assisted pyrolysis of hydrocarbon mixtures[16] and atomic H. The carbon nanopowders, stored in a reservoir, were carried by Ar streams and homogeneously delivered through a tubing system and a nozzle across the active area of the substrate. The nozzle can be rotated around its longitudinal axis in such a way that the streams of the carrier gas intersect at variable angles with the flux of atomic H generated by a Joule-heated Ta filament ($T = 2200 \pm 10$ °C). For the present experiments the intersection angle was fixed at 85°. The main process parameters were: H_2 flow rate, 200 sccm (standard cubic centimeter per minute); Ar flow rate, 30 sccm; substrate temperature, 900 °C; chamber operating pressure, 36 Torr.

The substrates were Si plates coated by a submicron dispersion of Fe nanoparticles, as previously reported,[17] and positioned at controlled distance with respect to the heated Ta filament. The distance, which represents a key parameter of the process, was fixed in the present experiment at 6 mm. For production of nanodiamond/nanotube systems the runs lasted 15 min. Some ad hoc experiments have been performed by changing the duration of the synthesis process in the range 1−15 min. This series of depositions was repeated twice, to have 2 sets of analogous samples to compare.

For the purpose of characterization, a field-emission type scanning electron microscope (FE-SEM) was used to investigate the morphology of the produced nanostructures and TEM images were obtained using a JEOL 2010 electron microscope operating at 160 kV.

The Raman spectra were taken at room temperature in the backscattering configuration using an Ar-ion laser beam (514.5 nm, laser power 10 mW) and a laser spot size of approximately 100 μm.[2]

The RHEED analysis was carried out using an AEI EM6G microscope equipped with a high-resolution diffraction stage (acceleration voltage 60 kV). The measurements were performed in selected area conditions, with the possibility of varying the angle of incidence of the electron beam with respect to the substrate surface. The diffraction patterns have been carefully processed using suitable image analysis software.

Results

Using the FE-SEM we have investigated the growth evolution of the nanostructures by analyzing frame-to-frame the images of the deposits generated under the same experimental conditions, but stopping the process at selected times. In Figure 2, one can observe the morphology of a series of deposits grown for 1, 2, and 6 min.

The information gathered from this analysis highlights a number of interesting features. First of all it is evident that, under our experimental conditions, the process of nanotube synthesis is characterized by a very high growth rate. The image of Figure 2a reveals, after only 1 min from the process commencement, the presence of rather long (about 3 μm) nanotubes. The nanotubes are assembled in winding thin bundles (diameter <120 nm). Many unreacted carbon nanoparticles are still present at this stage. After 2 min the substrate is covered by a denser deposit of assembled

(8) Baik, E. S.; Baik, Y. S.; Lee, S. W.; Jeon, D. *Thin Solid Films* **2000**, *377*, 295.
(9) Baik, E. S.; Baik, Y. S.; Jeon, D. *J. Mater. Res.* **2000**, *15*, 923.
(10) Ando, Y.; Nishibayashi, Y.; Sawabe, A. *Diamond Relat. Mater.* **2004**, *13*, 633.
(11) Masuda, H.; Yanagishita, T.; Yasui, K.; Nishio, K.; Yagi, I.; Rao Y. N.; Fujishima, A. *Adv. Mater.* **2001**, *13*, 247.
(12) Chih, Y. K.; Chen, C. H.; Hwang, J.; Lee A. P.; Kou, C. S. *Diamond Relat. Mater.* **2004**, *13*, 1614.
(13) Sun, L. T.; Gong, J. L.; Zhu, Z. Y.; Zhu, D. Z.; He, S. X.; Wang, Z. X.; Chen, Y.; Hu, G. *Appl. Phys. Lett.* **2004**, *84*, 2901.
(14) Sun, L. T.; Gong, J. L.; Zhu, D. Z.; Zhu, Z. Y.; He, S. X. *Adv. Mater.* **2004**, *16*, 1849.
(15) Terranova, M. L.; Piccirillo, S.; Sessa, V.; Sbornicchia, P.; Rossi, M.; Botti S.; Manno, D. *Chem. Phys. Lett.* **2000**, *327*, 284.
(16) Botti, S.; Coppola, R.; Gourbilleau, F.; Rizk, R. *J. Appl. Phys.* **2000**, *88*, 3396.
(17) Orlanducci, S.; Sessa, V.; Terranova, M. L.; Rossi, M.; Manno, D. *Chem. Phys. Lett.* **2003**, *367*, 109.

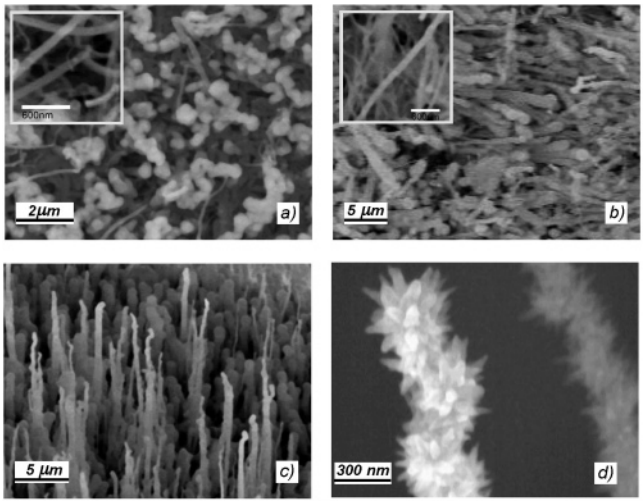

Figure 2. FE-SEM images of the deposits grown for a series of deposition times: (a) 1 min; (b) 2 min. The insets of (a) and (b) show the presence, after 1- and 2-min depositions, of nanotube bundles with smooth external surfaces; (c) 6 min; (d) 6 min: a close view of a bundle coated by embryo crystallites.

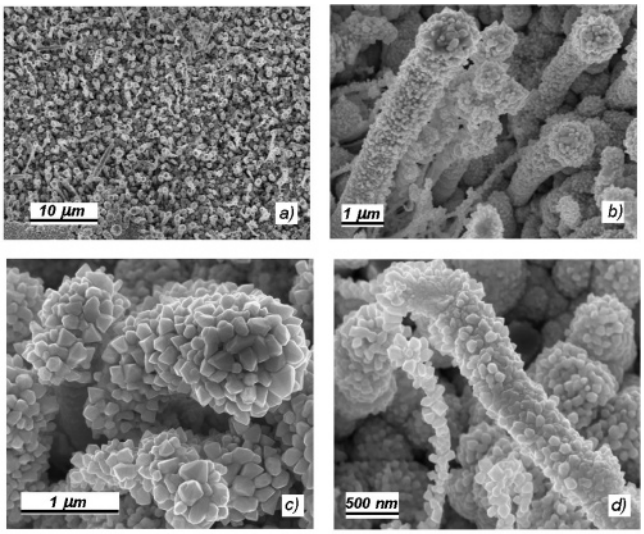

Figure 3. FE-SEM images showing: (a) the general view of a typical deposit; (b−d) the details of nanotube bundles covered by diamond nanocrystallites.

nanotubes, which have now reached a length of more than 10 μm (Figure 2b). The bundles begin to align parallel each other, and all evidence of residual carbon nanoparticles has gone. The insets of Figure 2a and b highlight the smoothness of the nanotube walls and the absence of any crystalline form on them. The situation is very similar for the synthesis time of 4 min. After 6 min the bundles begin to be vertically oriented (Figure 2c) and the FE-SEM images taken at higher magnification reveal the presence of nanosized objects (Figure 2d), which at this stage are found preferentially located on the surfaces of the larger bundles.

Figure 3a shows the top view of a typical deposit obtained after 15 min. With the exception of few detached bundles which lie parallel on the surface of the deposited material, the bundles are anchored and preferentially oriented at right angle with respect to the substrate, although not perfectly aligned. The FE-SEM view in Figure 3b shows that the diamond coverage is complete along the whole length of the

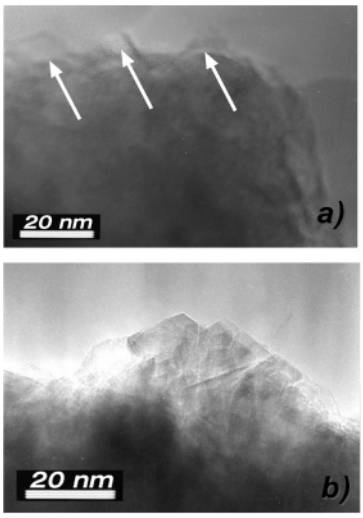

Figure 4. TEM images taken on the external edge putting in evidence the morphological shape of diamond grains covering the underlying tubular structures. The white arrows in (a) indicate secondary grain growth.

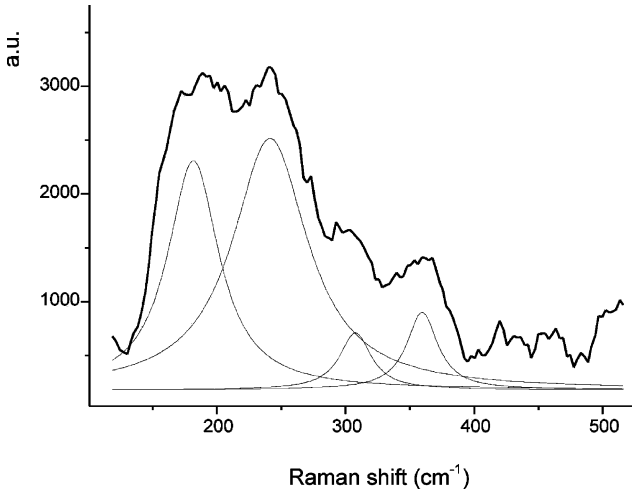

Figure 5. Raman spectrum in the RBM region of single-walled carbon nanotubes, obtained from the sample grown for 15 min. The dotted lines have been derived by curve fitting of the spectrum to Lorentzian lines after background subtraction.

tubes. The thickness and external diameter of these tubes range approximately from 100 up to 800 nm. At higher magnifications (Figure 3c and d) one notes that the wires are coated by grains with diameters ranging approximately between 20 and 100 nm, with well-defined crystalline facets.

The TEM observations, carried out on the longitudinal edge of isolated tubes, reported in Figure 4a and b, illustrate the crystalline features of the diamond grains covering the underlying tubular structures. The arrows in Figure 4a indicate the presence of a secondary grain growth characterized by a pyramidal morphology.

Figure 5 reports the Raman spectrum taken from the 15-min grown deposit shown in Figure 3a. The signals detected in the investigated low energy spectral region are associated with the A_{1g} radial breathing mode (RBM) of the C atoms within the structure. This feature is known to represent the fingerprint of the single-walled carbon nanotubes,[18−19] and is not observed in any other structures, such as nanofibers or wires. The analysis of the spectral features detected in the RBM region indicates that the tubular structures underly-

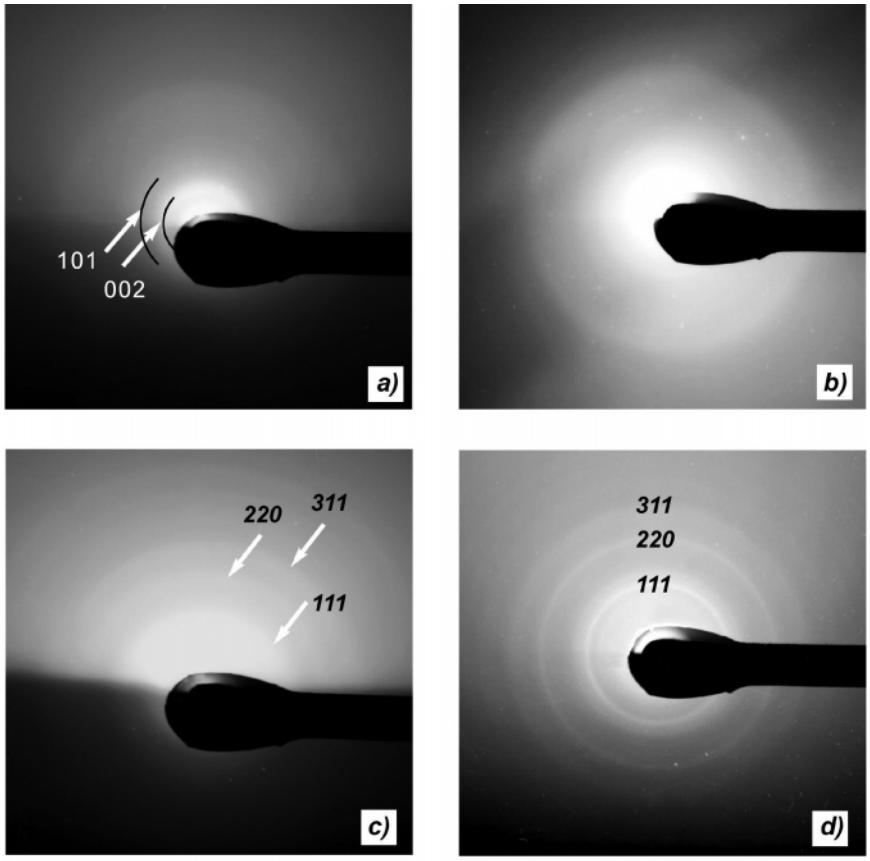

Diamond			Graphite		
$d_{spacing}$(Å)	hkl	I/I_0	$d_{spacing}$(Å)	hkl	I/I_0
2.0592	111	100.00	3.348	002	100
1.2610	220	28.10	2.127	100	3
1.0754	311	16.68	2.027	101	15
0.8916	400	1.98	1.795	102	3
0.8182	331	2.38	1.674	004	6
07280	422	2.34	1.5398	103	4
0.6864	511	1.11	1.1280	104	1
0.6305	440	0.49	1.1529	110	4
0.6029	531	0.75	1.1333	112	6

e)

Figure 6. Electron diffraction patterns of samples obtained from the deposition processes lasting 1 min (a), 2 min (b), 6 min (c), and 15 min (d). The images have been taken in the typical TEM configuration used for RHEED analysis. The particular morphological features (shape and size) of the observed samples made it possible to achieve ED pattern in transmission conditions (particularly evident in case of (b) and (d). The white arrows indicate: in (a) the diffraction rings produced by the presence of graphitic nanoparticles; in (c) the diffraction signals belonging to the *Fd*3*m* diamond phase; the indexing for the observed Debye's rings is also reported. (e) Interplanar distances with corresponding indexing and relative intensities for diamond and graphite phases (refs 21 and 22).

ing the external coating are mainly formed by self-assembled SWNTs.[18−19] The fine structure of the spectrum, evidenced by a line shape analysis using Lorentzian curves, shows two more intense signals at 183 and 242 cm^{-1}, whereas other weak features are detected at 310 and 350 cm^{-1}. It is also important to note that none of the spectra of the 6, 8, 10, or 15 min samples show the typical Raman signature of diamond at 1332 cm^{-1}. This is not unexpected because others have shown that a high degree of diamond surface hydrogenation can drastically reduce the Raman emission efficiency for the diamond phase, as demonstrated in ref 20. Moreover it must be considered that in the samples described here, the Raman signals are in part a function of the sample

(18) Rao, A. M.; Richter, E.; Bandow, S.; Chase, B.; Eklund, P. C.; Williams, K. A.; Fang, S.; Subbaswamy, K. R.; Menon, M.; Thess, A.; Smalley, R. E.; Dresselhaus, G.; Dresselhaus, M. S. *Science* **1997**, *275*, 187.

(19) Saito, R.; Dresselhaus, G.; Dresselhaus M. S. *Physical Properties of Carbon Nanotubes*; Imperial College Press: London, 1998.

(20) Maillard-Schaller, E.; Kuettel, O. M.; Diederich, L.; Schlapbach, L.; Zhirnov, V. V.; Belobrov, P. I. *Diamond Relat. Mater.* **1999**, *8*, 805.

volume, in which the diamond phase is only a small fraction. Therefore, although Raman is invaluable in definitely identifying the presence of SWNTs (via the signature RBMs), alternative techniques have been employed in the identification of the external crystalline deposits.

Further information on the structure of the tubular deposits has been obtained by means of RHEED. To detail the growth sequence of the various nanostructures, we took full advantage of the possibility of performing the RHEED analysis with an e-beam that could be driven to interact at a very glancing angle with the outermost part of the protruding deposit, thus obtaining diffraction signals in transmission conditions.

Figure 6 shows the RHEED pattern of the deposits shown in Figures 2 and 3 along with the interplanar distances and the calculated relative intensities[21,22] of graphite and diamond phases. The diffraction patterns of diamond and graphite present only a few common lines corresponding to similar interplanar distances, but these lines are characterized by remarkable differences in the relative intensities. Therefore, this technique allows easy and reliable identification of the two phases.

In the case of the sample produced by a deposition process lasting 1 min and shown in Figure 2a, the Debye's patterns (Figure 6a) were identified[15] as a superposition of signals due to both randomly dispersed nanotubes and graphitic nanoparticles (rings slightly elongated in the transversal direction, indicated by white arrows). On increasing the deposition time up to 2 min (Figure 6b), the signals due to the graphitic phase disappear and only the signals attributed to the presence of single-walled nanotubes remain. The wide broadening of the diffraction signals in Figure 6b led us to deduce that we are in the presence of single-walled structures and to exclude the possibility that the ED signals could be generated by multiwalled structures, nanorods, nanofibers, or nanowires (in agreement with the Raman RBM results).The RHEED patterns do not change appreciably for the sample obtained after 4 min. When RHEED analysis was performed on samples grown for 6 min (Figure 6c), an additional set of Debye's rings was detected (indicated with white arrows in Figure 6c). The indexing of the diffraction patterns and matching with literature data facilitated the identification of a standard diamond lattice (*Fd*3*m* space group),[21] whereas the broadening of the rings was ascribed to a morphology characterized by nanosized grains. The weakness of the diffraction signals belonging to the diamond phase may be explained by considering that (as mentioned above) the outermost crystalline deposit is only a fraction (and probably not the more relevant one at this stage of growth) of the material interacting with the e-beam.

The features of the RHEED pattern remain substantially unchanged for samples grown for 8 min. Finally, for the deposits obtained after 15 min the RHEED response (Figure 6d) shows the almost complete disappearance of the features related to the tubular nanostructures and the presence of well-defined diffraction signals belonging to the polycrystalline diamond phase. Overall, these results demonstrate a gradual disappearance of signals related to the presence of carbon nanotubes and the appearance of diffraction signals belonging to a crystalline phase. The fact that the diffraction pattern ascribed to the nanotubes tend to vanish when a complete coverage of diamond crystallites has been achieved is likely due to the fact that (under the present diffraction conditions), the probed depth is expected to be within approximately 10 nm; considerably less than the diameter of the diamond nanocrystals of 20−100 nm.

It is to be noted that the indexing of the diffraction signals of Figure 6 excludes the possibility that crystalline phases different from the two allotropic forms of carbon could be present in the tubular structure. All the possible Fe or Fe−carbide phases, whose presence could be hypothesized considering the synthesis procedures, belong to space groups with interplanar distances and relative intensities quite different and not compatible with the experimentally observed values. In full agreement with this remark, Auger spectroscopy (performed ex-situ on the deposits) did not reveal signals that could be attributed to the presence of any carbides phase.

Overall, the RHEED observations appear fully coherent with the information achieved by FE-SEM regarding the structural/morphological evolution of the two carbon-based materials produced during the same run. In particular the possibility of achieving electron diffraction patterns under transmission-like conditions clearly indicates that the crystalline material is not deposited on a 2D-substrate but is present on the edges of a 1D-structure (i.e., the nanotube bundles).

All the characterization techniques indicate that, for deposition times shorter than 6 min, the deposits are similar to those obtained in some previous experiments[17] and consist of bundles formed by assembled nanotubes. Only in the case of prolonged deposition times was the growth of a second nanocrystalline phase detected. The analysis of the structures grown for times varying between 1 and 15 min provides a clear description of the overall process and also indicates the growth sequence of the two types of nanostructured carbon, namely nanotubes and nanodiamond. The deposits shown in Figures 2c, 2d, and 3 actually result from two independent processes, the first one being the synthesis of the nanotubes, and the second one being the growth of diamond nanocrystallites onto the already-grown tubular structures.

Discussion

Despite the fact that atomic H is known to etch sp^2-bonded carbon during CVD treatments, the growth of diamond directly onto graphitic substrates is not unheard of.[23−28] As

(21) ICCD Database PDF 06-0675; CDF 037638.
(22) Rossi, M.; Vitali, G.; Terranova, M. L.; Sessa, V. *Appl. Phys. Lett.* **1993**, *63*, 2765.
(23) Mehandru, S. P.; Anderson, A. B.; Angus, J. C. *J. Phys. Chem.* **1992**, *96*, 10978.
(24) Li, Z.; Wang, L.; Suzuki, T.; Argiotia, A.; Pirouz P.; Angus, J. C. *J. Appl. Phys.* **1993**, *73*, 711.
(25) Lambrescht, W. R. L.; Le, C. H.; Segali, B.; Angus, J. C.; Li, Z.; Sunkara, M. *Nature* **1993**, *364*, 607.
(26) Suzuki, T.; Yagi, M.; Shibuki, K.; Hasemi, M. *Appl. Phys. Lett.* **1994**, *65*, 540.
(27) Regel, L. L.; Wilcox, W. R. *J. Mater. Sci. Lett.* **2000**, *19*, 455.
(28) Moran, M. B.; Klemm K. A.; Johnson, L. F. Diamond Film Deposition on Graphite; U.S. patent 5,654,044, 1997.

early as 1992, Angus and colleagues reported the nucleation and growth of diamond particles on the basal plane of graphite in the presence of atomic hydrogen and hydrocarbon gases, using a traditional microwave plasma CVD technique. Later in 1994 Suzuki et al.[26] reported the direct growth of faceted diamond particles on graphite flakes, showing that the diamond nucleated at the edge of the graphite flakes, with growth proceeding along the edges; clearly favoring the defective regions of the flakes. This work was confirmed in subsequent studies; most recently Regal and Wilcox have reported the deposition of faceted diamond on graphite under hydrogen-rich conditions, at pressures between 30 and 60 Torr with a substrate temperature of 750 °C, using a more innovative approach.[27]

On the basis of these studies (along with others mentioned above) and our reported results we can try to delineate the dynamics of the entire process. At the onset of the synthesis runs, etching of the source carbon nanoparticles by atomic H causes formation of excited C atoms and clusters in gas phase. At this stage the basic steps controlling the growth process of nanotubes are the condensation and self-assembly of sp^2-coordinated carbon clusters into nanoscale graphitic flakes, followed by the metal-catalyzed closing and wrapping of such nanoaggregates. The tubular network continues to grow by further additions of C clusters produced by gas-phase condensation and the morphology of nanotube bundles resembles that typical of the nanotubes produced in previous experiments.[17,29,30]

The process can then follow two different routes, depending on the relative abundance of atomic H. When the concentration of atomic H is relatively low, as in the usual experiments of SWNT synthesis carried out in our laboratory, the formation of nanotubes continues following the scheme described above. Otherwise (under the same deposition conditions), the nanotubes begin to fall victim to attack by atomic H, via the creation of defective sites on the nanotube wall, and a different pathway opens.[14,25] Several researchers[26−28] demonstrated that sufficient atomic H impinging on graphitic surfaces forms C−H bonds (as mentioned above), able to disrupt locally the C−C sp^2 network and to create localized C−C sp^3 defects that can act as suitable sites for nucleation of diamond crystallites.[26]

On the basis of the paper by Ruffieux et al.[31] it has been argued[13] that the continuous hydrogenation of carbon nanotubes induces the clustering of sp^3-bonded C atoms. These arguments prompted us to perform first principle calculations on atomic H impinging on the external surfaces of carbon nanotubes.[32]

The results of these calculations (designed to investigate the effects of atomic hydrogen adsorbates on model (6,6) and (9,0) SWNTs) illustrated that certain absorption configurations may produce defects containing dangling carbon bonds, and promote the formation of suitable sites for nucleation.[32] Changes in the structure were examined with one, two, and three hydrogen atoms chemisorbed onto the outer side of each tube wall in specific configurations. Multiple hydrogen atoms were adsorbed in two different configurations, involving H-adsorption equidistant around one of the six-membered rings, or around the base of a triangular pyramid formed by three carbon atoms bound to the same carbon in the center. The latter (pyramid) configuration was found to be energetically favorable, in addition to offering the possibility of a dangling bond being formed in the center of the defect. To test the energetic favorability of the pyramid configuration, carbon atoms were adsorbed at the center of the defect and the absorption energy was compared with that obtained for a site on each SWNT far from the H-defect (pristine). In general, the carbon atom adsorption energies were found to be consistently lower at the pyramid site than at a pristine position; thus showing that (depending upon the adsorption configuration) such sp^3 defects may contain a dangling bond and produce a site ideal for the nucleation of diamond nanocrystals.[32]

Therefore, the intriguing production of nanotube arrays coated by diamond nanograins can be rationalized if one considers that these experiments have been carried out in the presence of an unusually high concentration of atomic H. The reduced distance between the substrate and the heated filament (6 mm instead of the usual 8 mm of other runs) leads to an increased amount of atomic H which reaches the active area of the CVD reactor.

It is to be noted that under the general conditions of our syntheses the building up of nanotubes occurs by progressive additions of carbon clusters on the top of the growing structure. This can be deduced from the fact that the Fe particles used to catalyze the synthesis are found at the starting end of the nanotubes.[17]

On the other hand, nucleation of diamond does not occur simultaneously along the whole length of the tube, as demonstrated by the relative dimensions of the grains deposited at the top and at the bottom of the cylindrical structures. A close look at the images of Figure 2 reveals that the grains at the top have typical sizes in the range 80−100 nm, whereas at the bottom the grain sizes are less than 20 nm. The difference in size also indicates that the H-induced processes leading to nucleation of the diamond nanocrystallites start from the top of the nanotubes. This means that as soon as the first diamond crystallites are formed, further top-growth of the nanotube is repressed, and that the initial coverage of the growing end by diamond nanocrystallites limits the further build up of nanotubes.

The preferential formation of the diamond nanocrystallites rather than graphitic particles (or continued nanotube growth) may be considered via thermodynamic arguments. As mentioned above, ab initio calculations and a model derived to compare the energetic stability of carbon nanomaterials as a function of size have shown[33] that diamond nanoparticles

(29) Terranova, M. L.; Sessa, V.; Orlanducci, S.; Rossi, M.; Manno, D.; Micocci, G. *Chem. Phys. Lett.* **2004**, *388*, 36.
(30) Wu, Z. Y.; Davoli, I.; Terranova, M. L.; Orlanducci, S.; Sessa, V.; Abbas, M.; Ibrahim, K.; Zhong, J.; Botti, S. *Phys. Script.* **2005**, (in press).
(31) Ruffieux, P.; Groening, O.; Bielmann, M.; Mauron, P.; Schlapbach, L.; Groening, P. *Phys. Rev. B* **2002**, *66*, 245416.
(32) Barnard, A. S.; Terranova, M. L.; Rossi, M. *Chem. Mater.* **2005**, *17* (3), 527−535.
(33) Barnard, A. S.; Russo, S. P.; Snook, I. K. *J. Chem. Phys.* **2003**, *118*, 5094.

are thermodynamically preferred over fullerenes beyond a diameter of approximately 1.9 nm. It has also been shown that in general, a sp^3-bonded particle core is preferable over an onion-like core over approximately 1.4 nm.[34] It is therefore reasonable to deduce that sp^2-bonded nodules or nanostructures forming at defect sites on the outer walls of the nanotubes considered herein will be unstable to the sp^2-to-sp^3 phase transition and, upon reaching a critical size, will rapidly transform into diamond nanoparticles.

The diamond growth proceeds thereafter, taking advantage of the surface supersaturation and localized carbon segregation produced by the etching of some of the nanotubes as well as that of the feeding C nanopowders. At this stage the nanotubes represent an adjunctive source of carbon species which favors the growth of the diamond phase, and the process is comparable to the deposition of nanodiamond onto carbon nanorods,[13] amorphous carbon,[35] or carbon fibers.[36]

The gradual increase of nanotube alignment and orientation toward a defined direction is thought to be due to the increasing rigidity of the emerging structures. A current hypothesis is that the growth direction of the evolving nanotubular objects is being governed at this stage by the lattice matching of diamond nanocrystals nucleating and growing at or near the substrate.

Another morphological feature to be pointed out is that the diamond nuclei do not coalesce forming a continuous layer of nanograins. On the contrary, the nanograins are found arranged as hanging objects which attach to the tubular substrates via a reduced portion of their base. The orientation of the diamond crystallites protruding from the substrate can be ascribed to a process of diamond nucleation that is preferentially located on the summit of relief structures generated by H-etching of the nanotubes. Some aspects of the present diamond deposition on tubular graphitic substrates present indeed similarities with that experienced when diamond was deposited onto glassy carbon substrates.[37] In that experiment the surface erosion of glassy carbon substrates during the early stage of the CVD process was found to dictate the final arrangement of diamond grains into bridge-like protruding aggregates.[37] Successive investigations indicated that the reactions of atomic H with glassy carbon[38] and carbon fibers[36] promote the formation of turbostratic carbon, sometimes dishomogeneously aggregated in the form of nodules.[38]

In this context one can deduce that the present organization of protruding nanodiamond grains is driven by a nucleation process occurring preferentially on prominent graphitic nodules acting as active sites. The growing diamond grains remain anchored to the substrate by the bottom facets, and exposure to the incoming feeding flux of C nanoparticles ensures further growth and moderates the final shape, resulting sometimes in slight elongation. The production of diamond with nanosized dimensions is due to growing embryonic crystallites having reduced final domain sizes owing to the very small radius of curvature of the substrates. One must also consider that, in contrast to conventional CVD experiments of diamond synthesis, in the present case the fundamental building blocks are not simple atomic species but rigid nanostructured units. The result is that the structure of the deposit is dramatically dependent on how such units can self-organize and attach to the nanotube walls.

Conclusions

In conclusion, the synthesis process reported here outlines for the first time a systematic method of preparing arrays of nanodiamond-coated carbon nanotubes. Both scientific interest and prospective technological applications motivates the interest in this new class of hybrid nanomaterials. It is indeed possible to imagine several intriguing uses for such strong and stable nano-objects that combine the two solid phases of C.

Considering that diamond is one of the most promising wide band gap semiconductors for various electronic devices, with an excellent potential due to its negative electron affinity (NEA),[39] these rigid rods are expected to find applications as micro- and nanosized cold-cathode devices, miniaturized cathode-ray tubes, and light-emitting displays, but also applications in micromechanics and nanosized sensing could be envisaged.[40−41]

However, it must be considered that important problems remain to be addressed to reach the complete control of the growth modes for both the inner nanotube and the outermost diamond phases. One fundamental point is certainly to understand the mechanism of each step of a multi-stage, complex process where both chemical reactions and surface structural modifications play a key role. As an example, a deep knowledge of the processes of nanotube self-alignment and orientation following diamond growth is strongly needed to fully exploit potential opportunities for nanotechnology.

Although we have examined the transformation of our deposits from pure nanotubes to the final complicated hybrid material, a difficulty experienced in these experiments is that the resulting nanostructures are detected only after the formation steps have been completed. The rationale for stringent interpretation of the underlying phenomena can consequently be provided only by the use of theoretical tools, such as simulations, quantum mechanics, and molecular dynamics. We hope that the findings of the current research could trigger studies along this direction.

Acknowledgment. This work has been partially supported by the U.S. Department of Energy, Basic Energy Sciences, under contract W-31-109-ENG-38, and by the Italian MIUR through the FIRB National Program.

CM0502018

(34) Barnard, A. S.; Russo, S. P.; Snook, I. K. *Phys. Rev. B* **2003**, *68*, 073406.
(35) Singh, J. *J. Mater. Sci.* **1994**, *29*, 2761.
(36) Rossi, M.; Terranova, M. L.; Piccirillo, S.; Sessa, V.; Manno, D. *Chem. Phys. Lett.* **2005**, *402*, 340.
(37) Terranova, M. L.; Polini, R.; Sessa, V.; Braglia, M.; Cocito, G. *Diamond Relat. Mater.* **1992**, *1*, 966.
(38) Terranova, M. L.; Sessa, V.; Rossi, M. *Chem. Phys. Lett.* **2001**, *336*, 405.
(39) Pierson, H. O. *Handbook of Carbon, Graphite, Diamond and Fullerenes—Properties, Processing and Applications*; Noyes Publications: Park Ridge, NJ, 1993.
(40) Shenderova, O. A.; Areshkin, D.; Brenner, D. W. *Mater. Res.* **2002**, *6*, 11.
(41) Shenderova, O. A.; Areshkin, D.; Brenner, D. W. *Mol. Simul.* **2003**, *29*, 259.